Communications in Physics, Vol. 33, No. 4 (2023), pp. 411-420
DOI: https://doi.org/10.15625/0868-3166/18883

Structure optimization of large-solid-core photonic crystal fibers based on $Ge_{20}Sb_5Se_{75}$ for optical applications

Ngoc Vo Thi Minh[1], **Danh Nguyen Thanh**[2], **An Nguyen Manh**[3], **Tham Tran Hong**[4], **Van Thuy Hoang**[1], **Lanh Chu Van**[1] **and Hieu Van Le**[4,†]

[1]*Department of Physics, Vinh University, 182 Le Duan, Vinh City, Vietnam*

[2]*A Sanh High School, Gia Lai Province, Vietnam*

[3]*Faculty of Technology and Engineering, Hong Duc University, 565 Quang Trung Street, Thanh Hoa City, Vietnam*

[4]*Faculty of Natural Sciences, Hong Duc University, 565 Quang Trung Street, Thanh Hoa City, Vietnam*

E-mail: †levanhieu@hdu.edu.vn

Received 12 September 2023; *Accepted for publication 29 November 2023*
Published 18 December 2023

Abstract. *This paper presents a new design of $Ge_{20}Sb_5Se_{75}$ large-solid-core- square lattice photonic crystal fiber (PCF) with the first ring of air hole near the core removed. Using the full vector finite element method for anisotropic perfectly matched layers, we numerically examine the dispersion characteristics of the PCF as a function of the wavelength in the mid-infrared range. The results reveal that photonic crystal fibers exhibit a variety of dispersion properties, including all-normal and anomalous dispersion, featuring one or two zero dispersion wavelengths (ZDWs). Based on our numerical simulations, we propose two structures with optimal dispersion characteristics. These designs have small lattice constants ($\Lambda = 1.0$ μm; $\Lambda = 1.5$ μm) and low fill factors ($d/\Lambda = 0.3$; $d/\Lambda = 0.35$). These proposed PCFs could be candidates for many optical applications as supercontinuum generations source.*

Keywords: Photonic crystal fiber (PCF); dispersion characteristics; square lattice; chalcogenide, $Ge_{20}Sb_5Se_{75}$; effective mode area; confinement loss; optical applications.

Classification numbers: 42.55.Tv; 42.60.Jf; 77.22.Gm; 77.84.Bw.

1. Introduction

Photonic crystal fibers (PCFs), also known as micro-structured fibers or holey fibers, were first introduced in 1996 by Russell and his colleagues [1]. Over the last two decades, PCFs have

garnered significant attention due to their special and unique properties that go beyond traditional design and construction principles. They serve as a testament to the amalgamation of fundamental principles and advanced technological prowess, offering an exceptional platform for exploring the interaction between light and matter. This exploration spans a diverse landscape of applications, each holding the promise of unlocking new frontiers. PCFs possess remarkable characteristics, including high numerical aperture, strong birefringence, extremely large mode areas, and the ability to operate in single mode over a broad spectrum [2–4]. More recently, PCFs have transitioned from the confines of the laboratory to find utility in various fields such as optical communication, fiber light sources, fiber optic sensors, non-linear devices, and opto-fluidic devices [5–7]. Moreover, these fibers play a crucial role in the development of broad supercontinuum (SC) sources [8–10], which have found applications in a wide range of fields, including optical coherence tomography, optical metrology, and spectroscopy [11–13].

While advancing fiber optics, by manipulating the structural parameters and material properties of PCFs, researchers are able to finely adjust optical characteristics such as dispersion, effective mode refractive index, effective mode area, nonlinear coefficient, confinement loss, transmission spectrum, etc. The most commonly used lattices are circular, square, and hexagonal lattices. Each lattice bears a set of advantages and disadvantages, creating a variety of innovative designs. PCFs with hexagonal lattice structures excel in precise dispersion control. In contrast, circular lattice PCFs offer simplicity and ease of manufacturing with a small effective mode area. In particular, square lattice PCFs have low confinement loss and facilitate efficient long-distance light transmission. They provide polarization maintenance and compact integration into small optical systems [14–17]. So far, the PCFs with a solid core with the first ring removed has not been given much consideration yet. By eliminating more air holes in the core region, it is possible to fabricate a large-solid core PCF. These fibers are not only easy to coupling, but also withstand high power, simple fabrication, and high numerical aperture making them particularly suitable for applications such as high power supply, fiber amplifiers, fiber lasers and SC generations [14, 18, 19].

In terms of materials, there has been a departure from the traditional fused-silica PCFs with the limitation being its low nonlinear refractive index and its wavelength limit does not exceed 2.0 μm [16, 20]. Instead, researchers have recently injected liquid with a high nonlinear refractive index into the core, air holes, or used chalcogenide glass as the substrate material. Chalcogenide glasses have the additional virtue of being vitreous in nature, which enables them to be fiber-drawn. This distinctive property makes them among the select few materials capable of transmitting for far and mid-infrared light [21–23]. Chalcogenide glasses are multicomponent inorganic materials mainly composed of elements such as S, S, Te, As, Sb, Ge, and Si [24–26]. Se-based system such as Ge–Se has attracted much attention due to its wide range of applications in optoelectronic and thermal electric device fabrication [27]. With the addition of third element such as Sb to Ge–Se system, there are cross-linkages between the chains which strengthen the material [21]. The ternary Ge-Sb-Se chalcogenide system is of special interest for medical applications since it is believed to be less hazardous than its arsenic-containing equivalent.

In this paper, we proposed PCFs made of $Ge_{20}Sb_5Se_{75}$ chalcogenide for SC generation in the mid-IR region. The selected $Ge_{20}Sb_5Se_{75}$ chalcogenide introduce the rather good thermal, mechanical, chemical characteristics, and transparency in the 2.0-16.0 μm wavelength range [28–31]. In this work, the square lattice solid-core PCFs were studied with various lattice constant Λ and filling factor $f = d/\Lambda$ (d is diameter of air holes). In particular, the first air-hole ring near

the core has been removed to obtain a large core while controlling dispersion and other optical properties. From there, two optimal structures ($\Lambda = 1.0$ μm and $f = 0.35$; $\Lambda = 1.5$ and $f = 0.35$) with flat normal and anomalous dispersion have been proposed for the analysis of effective mode area, nonlinear characteristics, and confinement loss PCFs by using the finite-difference eigenmode method.

2. Theoretical foundations and numerical modeling

The purpose of this section is to construct a suitable high-nonlinearity glass structure that allows for the adjustment of optical property parameters. To achieve this, we use Lumerical Mode Solutions software to create PCFs with seven rings of air holes (the first-inner-ring air holes have been removed) organized in a square lattice (Fig. 1). The diameter of the air holes is d and the filling factor d/Λ changes in 0.05 increments from 0.2 to 0.8. The core diameter is obtained by the formula: $D_c = 4\Lambda - d$, where the lattice constant is varied from 1.0 μm to 2.5 μm in 0.05 increments. For this formula, the core is large enough for future experimental purpose, fabrication. In addition, it ensures the technological feasibility of the considered structures. In fact, in small-core PCF models, it is extremely difficult to couple with ordinary optical fibers. Thus, constructing fibers with a large core while maintaining optimal optical characteristics is an innovation and a significant achievement of contemporary designs.

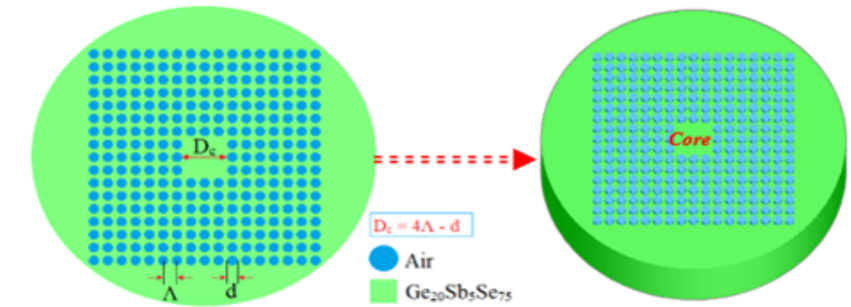

Fig. 1. Geometrical structure diagram of $Ge_{20}Sb_5Se_{75}$ solid-core PCF.

With the above design, we have specific parameters for the 52 fiber structures shown in Table 1. PCF with the smallest core diameter is 3.2 μm, PCF with the largest core diameter is 9.5 μm and the air hole diameter is from 0.2 μm to 2.0 μm. These sizes are quite favorable for practical PFC production purposes.

The refractive index characteristics modeled obeying the Sellmeier equation and given by the formula:

$$n(\lambda) = \sqrt{A_1 + \frac{B_1\lambda^2}{\lambda^2 - C_1} + \frac{B_2\lambda^2}{\lambda^2 - C_2} + \frac{B_3\lambda^2}{\lambda^2 - C_3}}, \tag{1}$$

where B_i and C_i are Sellmeier coefficients and λ is the wavelength. With the background materials chosen $Ge_{20}Sb_5Se_{75}$, the Sellmeier's coefficients are presented in Table 2.

Table 1. Parameters for the PCF structures are designed to perform simulations.

$\Lambda = 1.0\ \mu$m													
d/Λ	0.2	0.25	0.3	0.35	0.4	0.45	0.5	0.55	0.6	0.65	0.7	0.75	0.8
d	0.2	0.25	0.3	0.35	0.4	0.45	0.5	0.55	0.6	0.65	0.7	0.75	0.8
D_c	3.8	3.75	3.7	3.65	3.6	3.55	3.5	3.45	3.4	3.35	3.3	3.25	3.2
$\Lambda = 1.5\ \mu$m													
d/Λ	0.2	0.25	0.3	0.35	0.4	0.45	0.5	0.55	0.6	0.65	0.7	0.75	0.8
d	0.3	0.375	0.45	0.525	0.6	0.675	0.75	0.825	0.9	0.975	1.05	1.125	1.2
D_c	5.7	5.625	5.55	5.475	5.4	5.325	5.25	5.175	5.1	5.025	4.95	4.875	4.8
$\Lambda = 2.0\ \mu$m													
d/Λ	0.2	0.25	0.3	0.35	0.4	0.45	0.5	0.55	0.6	0.65	0.7	0.75	0.8
d	0.4	0.5	0.6	0.7	0.8	0.9	1	1.1	1.2	1.3	1.4	1.5	1.6
D_c	7.6	7.5	7.4	7.3	7.2	7.1	7	6.9	6.8	6.7	6.6	6.5	6.4
$\Lambda = 2.5\ \mu$m													
d/Λ	0.2	0.25	0.3	0.35	0.4	0.45	0.5	0.55	0.6	0.65	0.7	0.75	0.8
d	0.5	0.625	0.75	0.875	1	1.125	1.25	1.375	1.5	1.625	1.75	1.875	2
D_c	9.5	9.375	9.25	9.125	9	8.875	8.75	8.625	8.5	8.375	8.25	8.125	8

Table 2. Sellmeier's coefficients for $Ge_{20}Sb_5Se_{75}$ [27].

Sellmeier's coefficients	**Values**
A_1	1
B_1	4.7610
B_2	0.06994
B_3	0.8930
C_1 [μm^2]	0.0356
C_2 [μm^2]	0.6364
C_3 [μm^2]	491.72

The mode profiles associated with the eigenvectors and the propagation constants corresponding to the eigenvalues are calculated. Specifically, the chromatic dispersion coefficient (D) of PCFs was calculated from effective refractive index n_{eff} values versus the wavelength as Eq. (2) [16]:

$$D(\lambda) = -\frac{\lambda}{c}\frac{d^2\mathrm{Re}[n_{eff}]}{d\lambda^2}, \tag{2}$$

where Re [n_{eff}] is the real component of the effective refractive index at wavelength Λ for each mode and c is the vacuum light speed.

The following equation can be used to calculate the nonlinear coefficient (γ) of PCFs, which is dependent on the design of cladding structural parameters [15].

$$\gamma(\lambda) = \frac{2\pi}{\lambda}\frac{n_2}{A_{eff}}, \tag{3}$$

where n_2 is the nonlinear refractive index of $Ge_{20}Sb_5Se_{75}$, $n_2 = 4.29 \times 10^{-18} m^2.W^{-1}$ at the wavelength of 1550 nm [27] and A_{eff} is the effective mode area of the fiber. The mode area A_{eff} of the PCF is computed from [31]:

$$A_{eff}(\lambda) = \frac{\left(\iint |E(x,y)|^2 dxdy\right)^2}{\iint |E(x,y)|^4 dxdy}, \tag{4}$$

where $E(x,y)$ is the field distribution of the fiber mode. Besides, we can be interested in the confinement loss (L_c) calculated by the formula [31]:

$$L_c = 8.686\frac{2\pi}{\lambda}\mathrm{Im}[n_{\mathrm{eff}}(\lambda)], \tag{5}$$

where Im[n_{eff}] is the fictitious component of the n_{eff}.

3. Simulation results and analysis conclusion

Controlling the properties of photonic crystal fibers (PCFs), especially dispersion, lies at the heart of their versatile applications in modern photonics. Dispersion (D), the dependence of the phase velocity on the wavelength, is a critical parameter that influences the behavior of optical signals within a fiber. Here we have two types of dispersion: the normal dispersion state (D < 0) and the anomalous dispersion state ($D > 0$). The wavelength at which D is suppressed is called the zero-dispersion wavelength (ZDW). The dispersion-wavelength plots of the structures are shown in Fig. 2. The structural characteristics, such as the lattice constant Λ and the filling factor d/Λ govern the substantially wavelength-dependent dispersion. In all cases, we only calculate the fundamental mode with a wavelength range of 1.5–6.0 μm. Both all-normal and anomalous dispersions are obtained. In case the lattice constant is small, $\Lambda = 1.0$ μm (Fig. 2a), dispersion properties are quite diverse including all-normal and anomalous dispersion curves with one or two ZDWs. There are two all-normal dispersion curves with $d/\Lambda = 0.3$ and 0.35. The curve with $d/\Lambda = 0.35$ is closest to the zero dispersion line in the wavelength range of 2.49 μm - 4.0 μm.

In fact, the dispersion property is an important element in optical applications, particularly supercontinuum generation (SCG). Smaller dispersion magnitudes make optical signals more stable, reducing loss; flat dispersion fibers enable a broader SG to be produced. In this work. Our purpose is to design and simulate the PCFs for a supercontinuum generation at the selected pump wavelength of 3.0 μm with high coherence and a flat spectrum in the wide range of wavelengths from the near-IR to mid-IR regions. For this aiming, the optimization of the dispersion properties includes flatness, an indication of the dispersion characteristic, and the amount of difference between ZDW and pump wavelengths. Based on the simulation results, we proposed two PCFs structures, namely #F1, #F2 (Fig. 3). Fiber #F1 ($\Lambda = 1.0$ μm, $f = 0.35$, $D_c = 3.65$ μm) is designed to work in the all normal dispersion regions. This fiber has a flatness dispersion curve in the considered wavelength range. In addition, the fiber has a dispersion curve closest to the zero dispersion line, the maximum dispersion value is -8.32 ps/nm/km at 3.08 μm. For fiber #F2

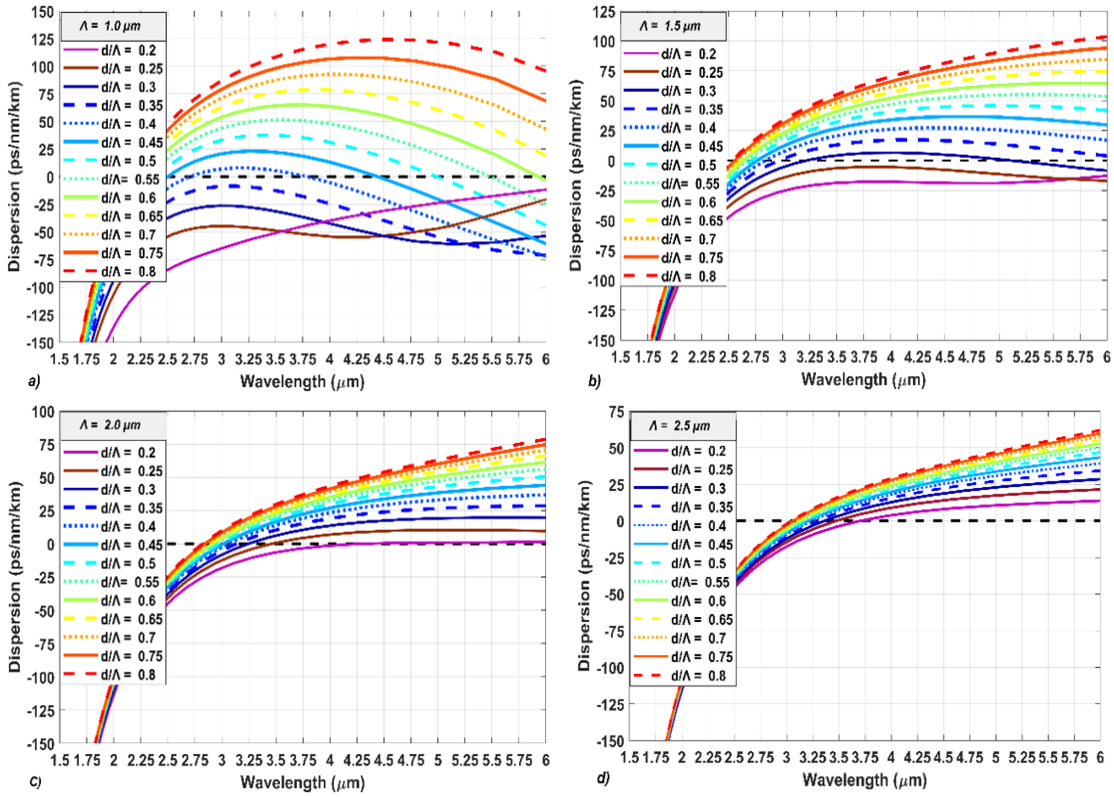

Fig. 2. The dispersion as a function of wavelength of PCFs with various filling factor ($f = d/\Lambda$): a) $\Lambda = 1.0$ μm, b) $\Lambda = 1.5$ μm, c) $\Lambda = 2.0$ μm, and d) $\Lambda = 2.5$ μm.

($\Lambda = 1.5$ μm, $f = 0.35$, $D_c = 5.475$ μm), it is expected to generate the supercontinuum generation in the anomalous dispersion. This fiber was chosen because it has a ZDW at 2.91 μm, which is the closest wavelength compared to the one pumped. The optical parameters of the optimal structures are shown in Table 3.

Table 3. The optical parameters of the optimal PCF structures.

#	d	D_c	ZDWs (μm)	flat-dispersion range (μm)	A_{eff} (μm^2)	L_c (dB/m)
#F1	0.35	3.65	-	$2.49-4.0$	$8.83-11.77$	$0.00024-3.16$
#F2	0.525	5.475	2.91	$2.91-6.0$	$18.17-27.54$	$2.1.10-6-1.41$

As Λ increases to 1.5 μm (Fig. 2b), both of the above dispersion lines become anomalous dispersion with two ZDWs ($d/\Lambda = 0.3$), and one ZDWs ($d/\Lambda = 0.35$). They are all flat and close to the zero dispersion line with a wide spectral range. With $\Lambda = 2.0$ μm and 2.5 μm (Fig. 2c and d), the increase of the filling factor d/Λ and Λ causes the dispersion curves to shift upwards, beyond the zero dispersion curve. In this case, we achieve anomalous dispersion for all structures.

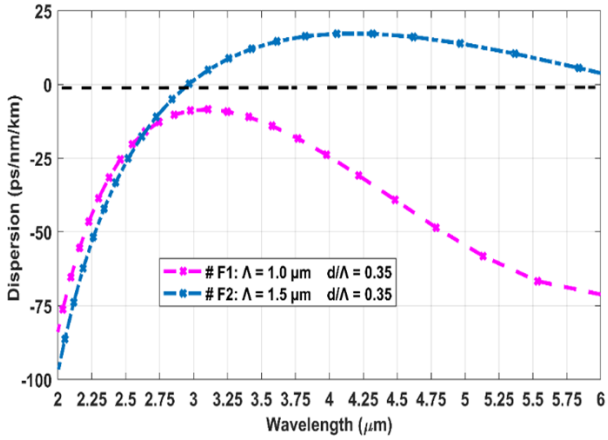

Fig. 3. The dispersion properties of the proposed PCFs.

Furthermore, for $\Lambda = 2.0\ \mu$m, the increase of the filling factor d/Λ increases the value of the dispersion at each defined wavelength.

Next, the effective mode area and nonlinear coefficient of the optimized structures are also considered. The effective mode area increases linearly as a function of wavelengths. When the effective mode area of PCF is small, the nonlinear coefficient will be large, the nonlinear interaction will be strong, as shown in Fig. 4.

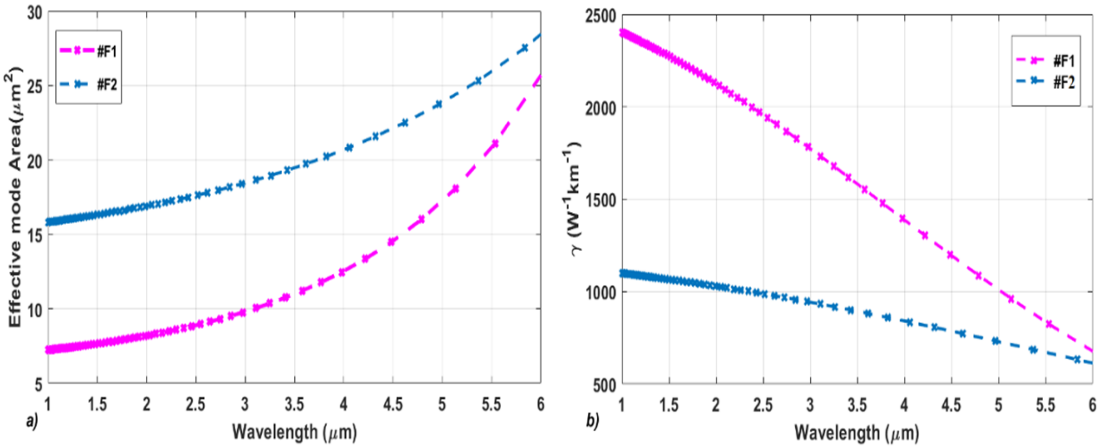

Fig. 4. The effective mode area and the nonlinear coefficients of the proposed fibers as a function of wavelength.

Figure 5 detected the confinement loss in proposed PCF structures. The results show that the losses maintain an overall tendency to increase with increasing wavelength. In addition, the structures we have chosen not only have near-zero dispersion, small gradients, the flat spectrum stretches in the infrared region but also their loss is small.

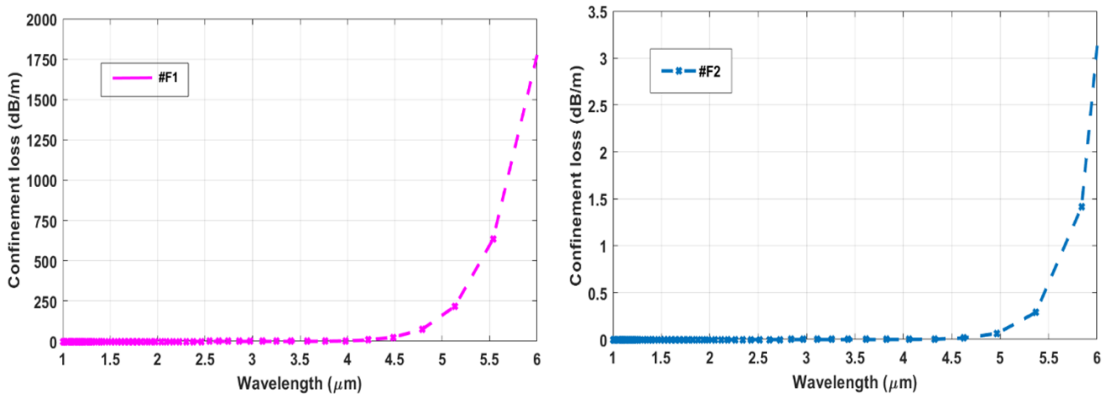

Fig. 5. Confinement loss as a function of wavelength for the proposed fibers.

Table 4. Comparison of the dispersion properties on the prospered PCFs and in several PCFs made of soft glass.

All-normal dispersion				
PCF	# F1	[32]	[33]	[31]
Substrate	$Ge_{20}Sb_5Se_{75}$	As_2Se_3	SiO_2	$Ge_{20}Sb_5Se_{75}$
Lattice type	Square	Square	Square	Hexagonal
Dispersion around the pump wavelength of 3.0 μm (ps.[nm.km]$^{-1}$)	-8.32	-10.972	-16.294	-4.52
Anomalous dispersion				
PCF	# F1	[32]	[33]	[31]
Substrate	$Ge_{20}Sb_5Se_{75}$	As_2Se_3	SiO_2	$Ge_{20}Sb_5Se_{75}$
Lattice type	Square	Square	Square	Hexagonal
Dispersion around the pump wavelength of 3.0 μm (ps.[nm.km]$^{-1}$)	1.16	10.9	2.03	3.56

Compared to recent publications such as studying square lattice structures with As_2Se_3 substrate [32] or SiO_2 substrate [33] or hexagonal lattice using $Ge_{20}Sb_5Se_{75}$ substrate [31] as show in Table 4. Fiber #F1 with all-normal dispersion has a dispersion curves closest 0 than fibers in [32, 33] and flatness dispersion curves than fibers in [31, 33]. In the case of fiber #F2, the fiber has the smallest dispersion value at the pump wavelength compared to the fibers in [31–33].

4. Conclusion

In this work, we have focused on studying and exploring the dispersion properties of the large–core-square lattice photonic crystal fibers based on the $Ge_{20}Sb_5Se_{75}$ compound. Their dispersion properties allow the creation of optical fibers with near-zero flat dispersion and wide dispersion: #F1 ($\Lambda = 1.0\ \mu$m, $f = 0.35$); #F2 ($\Lambda = 1.5\ \mu$m, $f = 0.35$), providing applications for SC sources. The first fiber #F1 ($\Lambda = 1.0\ \mu$m, $f = 0.35$, $D_c = 3.65\ \mu$m) is designed to work in the all normal dispersion region. This fiber has a flatness dispersion curves in the considered wavelength range. In addition, the fiber has a dispersion curve closest to the zero dispersion line, the maximum dispersion value is -8,32 ps/nm/km at 3.08 μm. For second fiber #F2 ($\Lambda = 1.5\ \mu$m, $f = 0.35$, $D_c = 5.475\ \mu$m), it is expected to generate the supercontinuum generation in the anomalous dispersion. This fiber was chosen because it has a ZDW at 2.91 μm, which is the closest wavelength compared to the one pumped. Another advantage of these fibers is that these fibers have larger core that allows couples to single-mode fiber with high coupling efficiency when considering an all-fiber SG system. The flexibility of these structures opens the door for a multitude of applications across diverse domains, including high-speed communications, ultrafast lasers and advanced sensors. It not only propels advancements in the field of optics but also enhances the potential of PCFs, expanding their practical applications.

Acknowledgments

This research is funded by Vietnam's Ministry of Education and Training (B2023-TDV-07), Hong Duc University (ĐT-2022-06).

References

[1] J. C. Knight, T. A. Birks, P. S. J. Russell and D. M. Atkin, *All-silica single-mode optical fiber with photonic crystal cladding*, Opt. Lett. **21** (1996) 1547.

[2] W. J. Wadsworth, R. M. Percival, G. Bouwmans, J. C. Knight, T. A. Birks, T. D. Hedley *et al.*, *Very high numerical aperture fibers*, IEEE Photonics Technology Letters **16** (2004) 843.

[3] T. Schreiber, F. Röser, O. Schmidt, J. Limpert, R. Iliew, F. Lederer *et al.*, *Stress-induced single-polarization single-transverse mode photonic crystal fiber with low nonlinearity*, Opt. Express **13** (2005) 7621.

[4] J. C. Knight, T. A. Birks, R. F. Cregan, P. Russell and J. P. De Sandro, *Large mode area photonic crystal fibre*, Electron. Lett. **34** (1998) 1347.

[5] P. Wan, L.-M. Yang and J. Liu, *All fiber-based yb-doped high energy, high power femtosecond fiber lasers*, Opt. Express **21** (2013) 29854.

[6] M. S. S. Ibrahim, M. S. M. Esmail, M. Tarek, A. Soliman, M. F. O. Hameed and S. Obayya, *Terahertz photonic crystal fiber for sensing the creatinine level in the blood*, Opt. Quantum Electron. **55** (2023) 767.

[7] P. D. Rasmussen, J. Lægsgaard and O. Bang, *Chromatic dispersion of liquid-crystal infiltrated capillary tubes and photonic crystal fibers*, J. Opt. Soc. Am. B **23** (2006) 2241.

[8] L. Chu Van, B. Tran Le Tran, T. Dang Van, N. Vo Thi Minh, T. Nguyen Thi, H. Phuong Nguyen Thi *et al.*, *Supercontinuum generation in highly birefringent fiber infiltrated with carbon disulfide*, Opt. Fiber Technol. **75** (2023) 103151.

[9] L. C. Van, N. V. T. Minh, B. T. L. Tran, T. D. Van, P. N. T. Hong, T. D. Mai *et al.*, *Broadband supercontinuum generation in cascaded tapered liquid core fiber*, Opt. Commun. **537** (2023) 129441.

[10] V. T. Hoang, Y. Boussafa, L. Sader, S. Février, V. Couderc and B. Wetzel, *Optimizing supercontinuum spectro-temporal properties by leveraging machine learning towards multi-photon microscopy*, Front. Photon. **3** (2022) 940902.

[11] A. Ghanbari, A. Kashaninia, A. Sadr and H. Saghaei, *Supercontinuum generation for optical coherence tomography using magnesium fluoride photonic crystal fiber*, Optik **140** (2017) 545.

[12] J. Woodward, A. Smith, C. Jenkins, C. Lin, S. Brown and K. Lykke, *Supercontinuum sources for metrology*, Metrologia **46** (2009) S277.
[13] I. Zorin, J. Kilgus, K. Duswald, B. Lendl, B. Heise and M. Brandstetter, *Sensitivity-enhanced fourier transform mid-infrared spectroscopy using a supercontinuum laser source*, Applied Spectroscopy **74** (2020) 485.
[14] A. Medjouri, L. M. Simohamed, O. Ziane and A. Boudrioua, *Analysis of a new circular photonic crystal fiber with large mode area*, Optik **126** (2015) 5718.
[15] N. V. Thi Minh, L. C. Van, P. N. Thi Hong, V. T. Hoang, H. Thi Nguyen and H. V. Le, *Supercontinuum generation in a square-lattice photonic crystal fiber using carbon disulfide infiltration*, Optik **286** (2023) 171049.
[16] B. T. Le Tran, T. N. Thi, N. V. Thi Minh, T. L. Canh, M. L. Van, V. C. Long *et al.*, *Analysis of dispersion characteristics of solid-core pcfs with different types of lattice in the claddings, infiltrated with ethanol*, Photonics Letters of Poland **12** (2020) 106–108.
[17] L. Van, T. Thi, D. Trong, B. T. Le Tran, V. T. M. Ngoc, V. Dang *et al.*, *Comparison of supercontinuum spectrum generating by hollow core pcfs filled with nitrobenzene with different lattice types*, Opt. Quantum Electron. **54** (2022) .
[18] W. Wong, X. Peng, J. McLaughlin and L. Dong, *Breaking the limit of maximum effective area for robust single-mode propagation in optical fibers*, Opt. Lett. **30** (2005) 2855.
[19] Y. Jeong, J. Sahu, D. Payne and J. Nilsson, *Ytterbium-doped large-core fiber laser with 1 kw continuous-wave output power*, in *Advanced Solid-State Photonics*, p. PDP13, Optica Publishing Group, 2004, DOI.
[20] H. L. Van, V. T. Hoang, T. L. Canh, Q. H. Dinh, H. T. Nguyen, N. V. T. Minh *et al.*, *Silica-based photonic crystal fiber infiltrated with 1,2-dibromoethane for supercontinuum generation*, Appl. Opt. **60** (2021) 7268.
[21] N. Sharma, S. Sharda, V. Sharma and P. Sharma, *Far-infrared investigation of ternary ge–se–sb and quaternary ge–se–sb–te chalcogenide glasses*, Journal of Non-Crystalline Solids **375** (2013) 114.
[22] L. Chu Van, T. Nguyen Thi, B. T. Le Tran, D. H. Trong, N. V. Thi Minh, H. Van Le *et al.*, *Multi-octave supercontinuum generation in as2se3 chalcogenide photonic crystal fiber*, Photonics and Nanostructures - Fundamentals and Applications **48** (2022) 100986.
[23] L. C. Van, H. V. Le, N. D. Nguyen, N. V. T. Minh, Q. H. Dinh, V. T. Hoang *et al.*, *Modeling of lead-bismuth gallate glass ultra-flatted normal dispersion photonic crystal fiber infiltrated with tetrachloroethylene for high coherence mid-infrared supercontinuum generation*, Laser Phys. **32** (2022) 055102.
[24] A. Seddon, *Chalcogenide glasses: a review of their preparation, properties and applications*, J. Non-Cryst. Solids **184** (1995) 44.
[25] W.-H. Wei, F. Liang, X. Shen and R. Wang, *Transition threshold in gexsb10se90-x glasses*, J. App. Phys. **115** (2014) .
[26] D. Jayasuriya, C. R. Petersen, D. Furniss, C. Markos, Z. Tang, M. S. Habib *et al.*, *Mid-ir supercontinuum generation in birefringent, low loss, ultra-high numerical aperture ge-as-se-te chalcogenide step-index fiber*, Opt. Mater. Express **9** (2019) 2617.
[27] N. Mi, B. Wu, L. Jiang, L. Sun, Z. Zhao, X. Wang *et al.*, *Structure design and numerical evaluation of highly nonlinear suspended-core chalcogenide fibers*, J. Non-Cryst. Solids **464** (2017) 44.
[28] J. Savage, P. Webber and A. Pitt, *An assessment of ge-sb-se glasses as 8 to 12μm infra-red optical materials*, J. Mater. Sci. **13** (1978) 859.
[29] A. Hilton and D. Hayes, *The interdependence of physical parameters for infrared transmitting glasses*, J. Non-Cryst. Solids **17** (1975) 339.
[30] M. Rechtin, A. Hilton and D. Hayes, *Infrared transmission in ge-sb-se glasses*, J. Electron. Mater. **4** (1975) 347.
[31] V. T. M. Ngoc, T. V. Thanh, C. T. H. Sam, D. V. Tran, Le Tran Bao an Trong, N. T. Thuy, L. V. Hieu *et al.*, *Optimization of optical properties of ge20sb5se75-based photonic crystal fibers*, Vinh Univ. J. Sci. **51** (2022) 12.
[32] D. V. Trong, L. T. B. Tran, H. T. A. Thu, N. T. Thuy and C. V. Lanh, *Study on dispersion characteristics of square solid-core photonic crystal fibers with as2s3 substrate*, Vinh Univ. J. Sci. **51** (2022) 44.
[33] T. B. T. Le, V. T. Dang, V. L. Chu, T. H. P. Nguyen, N. M. H. Trang, T. D. Hoang *et al.*, *Nonlinear characteristics of square solid-core photonic crystal fibers with various lattice parameters in the cladding*, Dalat University Journal of Science **13** (2022) 3.